DE GRUYTER Open Phys. 2019; 17:587–600

Research Article

Madiha Ghamkhar, Muhammad Nawaz Naeem, Muhammad Imran*, and Constantinos Soutis

Vibration Analysis of a Three-Layered FGM Cylindrical Shell Including the Effect Of Ring Support

https://doi.org/10.1515/phys-2019-0060
Received Jun 28, 2018; accepted Jul 27, 2019

Abstract: In this work, we study vibrations of three-layered cylindrical shells with one ring support along its length. Nature of material of the central layer is a functionally graded material (FGM) type. The considered FGM is of stainless steel and nickel. The internal and external layers are presumed to be made of isotropic material i.e., aluminum. The functionally graded material composition of the center layer is assorted by three volume fraction laws (VFL) which are represented by mathematical expressions of polynomial, exponential and trigonometric functions. The implementation of Rayleigh-Ritz method has been done under the Sanders' shell theory to obtain the shell frequency equation. Natural frequencies (NFs) are attained for the present model problem under six boundary conditions. Use of characteristic beam functions is made for the estimation of the dependence of axial modals. The impact of layer material variations with ring support is considered for many ring positions. Also the effect of volume fraction laws is investigated upon vibration characteristics. This investigation is performed for various physical parameters. Numerous comparisons of values of shell frequencies have been done with available models of such types of results to verify accuracy of the present formulation and demonstrate its numerical efficiency.

Keywords: cylindrical shell, functionally graded material, isotropic material, ring support, Sanders' shell theory, Rayleigh-Ritz method

PACS: 02.60.Cb; 68.35.Ja; 02.70.c

***Corresponding Author: Muhammad Imran:** Department of Mathematics, Government College University Faisalabad, Pakistan; Email: drmimranchaudhry@gcuf.edu.pk
Madiha Ghamkhar: Department of Mathematics, Government College University Faisalabad, Pakistan & Department of Mathematics and Statistics, University of Agriculture Faisalabad, Pakistan; Email: madiha_gm@yahoo.com
Muhammad Nawaz Naeem: Department of Mathematics, Government College University Faisalabad, Pakistan; Email: mnawaznaeem@gcuf.edu.pk
Constantinos Soutis: Aerospace Research Institute and Northwest Composites Centre, The University of Manchester, United Kingdom; Email: constantinos.soutis@manchester.ac.uk

1 Introduction

A cylindrical shell is a significant element in structural dynamics. Different mechanical aspects of such types of shells are studied for their practical applications, shell vibration is one of them. This investigation of these shells play a paramount part in the fields of technology, like pressure vessels, nuclear power plants, piping system and other marine and aircraft applications. Many researches [1–8] have been done the studies on vibrational performance of functionally graded (FG) cylindrical shells (CSs) and influence on the frequencies of layered shells due to edge conditions has been studied by Loy and Lam [9]. The core of all the previous research work has been elaborated by Love's thin shell theory. Furthermore Loy and Lam [10] gave an investigation of frequency characteristics of thin walled cylindrical shell (CS) under ring supports for several end conditions by using Sanders' shell theory and Ritz formulation. Xiang *et al.* [11] used Goldenveizer-Novozhilov theory of shells to determine the exact vibration solution of the same circular cylinders supported by multiple transitional rings. The state-space technique was applied to obtaine shell governing equations for shell splinter and the influences of edge conditions were attained. The effects on frequency parameters for different locations of ring supports were observed. The vibration behavior of open circular cylinders grounded on intermediary ring elastic support was analyzed by Zhang and Xiang [12]. They assessed the influence for number of intermediate ring assistances, their positions, associated boundary conditions and variations included angles on the behavior of the shells. Swaddiwudhipong *et al.* [13] explained the study of vibration of CSs with middle supports by applying the Ritz method to approximate their frequencies and mode shapes. An analysis of vibration frequency for a FG shell was done by Arshad *et al.* [14] with effect of different fraction laws by applying Love's first order shell theory. Another study about the frequency analysis of bi-layered CSs has been presented by the same authors in [15]. The shells were assembled from functionally graded materials (FGMs) as well as isotropic materials. The influences of particular shell configurations on NFs of cylinder-shaped shells were scrutinized. The solidity of the same shells made up of FG structure layer associated with axial load placed on the Winkler-Pasternak foundations was analyzed by Sofiyev and Avear [16]. Arshad *et al.* [17] explored vibration properties of bi-layered cylinder-shaped shell with both layers made up of FG layers by considering constant thickness. Law-II was exploited to study the material distribution of FGMs. They studied the effect on vibrations of double layered FG shell for various shell constraints, edge conditions and exchange the essential materials making FGMs. Zhang *et al.* [18] investigated the shell free vibrations for a number of edge conditions by using a differential quadrature type procedure. Naeem *et al.* [19] analyzed vibration behavior of the tri-layered FGM circular cylinders. They employed the Ritz method and used the Love's shell theory. Governing mathematical expression was in an integral form by considering the shell strain and kinetic energy relations. Axial modal dependence was examined with solution functions of beam equation. Arshad *et al.* [20] made a study of FG three-layered cylinder-shaped shells for free vibration under a ring support. Their work deals with the effect of ring supports, located at different positions along the length of cylinder-shaped shell for different edge conditions. The analysis was based on Love's thin shell theory. Rayleigh-Ritz formulation was employed to obtain solutions of the problem. The vibration response of tri-layered shells was investigated by Li *et al.* [21]. Ghamkhar *et al.* [22] studied vibration frequency analysis for three layered cylinder shaped shell with FGM central layer. The effect on shell vibrations for different thickness of the central layer were examined by them. The analysis was based on sander's shell theory and Ritz mathematical approach. Functionally graded material distribution was controlled with trigonometric volume fraction law.

In this work, vibration frequencies are analyzed for three layered cylindrical shells. These shells are assembled from three layers assuming that the central is made of functionally graded materials, internal and external layers remain isotropic type of materials. Material of the central layer is controlled by following volume fraction laws, polynomial (Law-I), exponential (Law-II) and trigonometric (Law-III). These laws are framed by polynomial, exponential and trigonometric functions. These laws vary the material composition in the radial (through-thickness) direction. This material variation yields a variety of frequency spectra. Stability of these shells is solidified by ring supports around the tangential directions. Sanders' thin shell theory is adopted for shell governing equations. These equations are solved by applying Rayleigh Ritz technique involving an energy variation functional. Axial deformation functions are estimated by the solution functions of beam equation. Such functions are taken to meet the edge conditions. An effect of layer thickness configurations is observed on shell natural frequencies. Results are obtained to examine the influence of ring supports at different positions along the shell length.

2 Theoretical considerations

Consider a cylinder-shaped shell sketched in Figure 1. Here length of the shell is denoted by$L$, thickness is denoted by H and the mean radius symbolized by$R$. They represent the shell geometrical quantities. A cylindrical coordinate system (x, θ, z) is framed at the shell middle reference surface with x, θ and z as the axial, angular and thickness coordinates respectively. Deformation displacement functions are designated by$u_1(x, \theta, t)$, $u_2(x, \theta, t)$ and $u_3(x, \theta, t)$ which denote the displacement deformations in the longitudinal, tangential and transverse directions respectively. The strain energy $\Im$ for a thin vibrating CS as in [10] is described below:

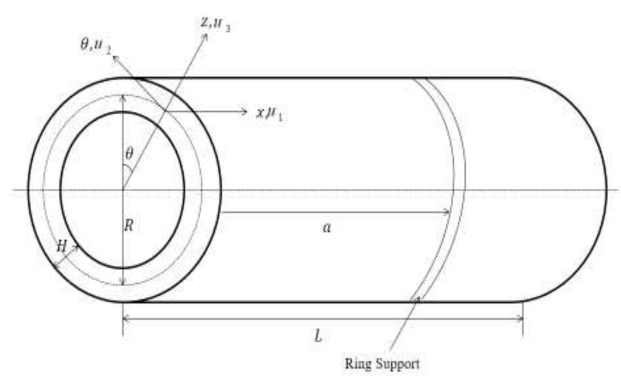

Figure 1: Geometry of CS with a ring support that its location varies along the length

$$\Im = \frac{1}{2}\int_0^L\int_0^{2\pi}\{K\}'[C]\{K\}Rd\theta dx \tag{1}$$

where

$$\{K\}' = \{\in_1, \in_2, \in_{12}, \kappa_1, \kappa_2, 2\kappa_{12}\} \tag{2}$$

and $\in_1$, $\in_2$ and $\in_{12}$ denote strains which are related to the reference surface and κ_1, κ_2 and κ_{12} represent curvatures. Prime ($'$) indicates the matrix transposition.
The entries of the matrix $[\mathbb{C}]$ are furnished as:

$$[\mathbb{C}] = \begin{pmatrix} x_{11} & x_{12} & 0 & y_{11} & y_{12} & 0 \\ x_{12} & x_{22} & 0 & y_{12} & y_{22} & 0 \\ 0 & 0 & x_{66} & 0 & 0 & y_{66} \\ y_{11} & y_{12} & 0 & z_{11} & z_{12} & 0 \\ y_{12} & y_{22} & 0 & z_{12} & z_{22} & 0 \\ 0 & 0 & y_{66} & 0 & 0 & z_{66} \end{pmatrix} \quad (3)$$

where x_{ij} represent the extensional, y_{ij}, coupling and z_{ij}, bending stiffness. ($i, j = 1, 2$ and 6). They are defined by the following formulas:

$$\{x_{ij}, y_{ij}, z_{ij}\} = \int_{-H/2}^{H/2} \mathbb{Q}_{ij} \left\{1, z, z^2\right\} dz \quad (4)$$

The reduced stiffness $\mathbb{Q}_{ij}$ for isotropic materials is stated as [10]:

$$\mathbb{Q}_{11} = \mathbb{Q}_{22} = E(1-\mu^2)^{-1}, \quad (5)$$
$$\mathbb{Q}_{12} = \mu E(1-\mu^2)^{-1}, \ \mathbb{Q}_{66} = E[2(1+\mu)]^{-1}$$

Here E represents the Young's modulus and μ denotes the Poisson ratio. The matrix $y_{ij} = 0$ for isotropic circular shaped CS and $y_{ij} \neq 0$ for a FG cylindrical shell; its value determined by the arrangement and properties of its constituent materials. After substituting the expressions from (2) and (3) in (1), $\Im$ is rewritten as:

$$\Im = \frac{1}{2}\int_0^L \int_0^{2\pi} \{x_{11} \in_1^2 + x_{22} \in_2^2 + 2x_{12} \in_1 \in_2 \quad (6)$$
$$+ x_{66} \in_{12}^2 + 2y_{11} \in_1 \kappa_1 + 2y_{12} \in_1 \kappa_2 + 2y_{12} \in_2 \kappa_1$$
$$+ 2y_{22} \in_2 \kappa_2 + 4y_{66} \in_{12} \kappa_{12} + z_{11}\kappa_1^2$$
$$+ z_{22}\kappa_2^2 + 2z_{12}\kappa_1\kappa_2 + 4z_{66}\kappa_{12}^2\} R d\theta dx$$

Following expressions are taken from [23] and written as

$$\{\in_1, \in_2, \in_{12}\} \quad (7)$$
$$= \left\{\frac{\partial u_1}{\partial x}, \frac{1}{R}\left(\frac{\partial u_2}{\partial \theta} + u_3\right), \left(\frac{\partial u_2}{\partial x} + \frac{1}{R}\frac{\partial u_1}{\partial \theta}\right)\right\}$$

$$\{\kappa_1, \kappa_2, \kappa_{12}\} = \left\{-\frac{\partial^2 u_3}{\partial x^2}, -\frac{1}{R^2}\left(\frac{\partial^2 u_3}{\partial \theta^2} - \frac{\partial u_2}{\partial \theta}\right), \quad (8)$$
$$-\frac{1}{R}\left(\frac{\partial^2 u_3}{\partial x \partial \theta} - \frac{3}{4}\frac{\partial u_2}{\partial x} + \frac{1}{4R}\frac{\partial u_1}{\partial \theta.}\right)\right\}$$

By substituting expressions (7) and (8) into equation (6), then $\Im$ becomes as:

$$\Im = \frac{R}{2}\int_0^{2\pi}\int_0^L \left[x_{11}\left(\frac{\partial u_1}{\partial x}\right)^2 + \frac{x_{22}}{R^2}\left(\frac{\partial u_2}{\partial \theta} + u_3\right)^2 \quad (9)\right.$$
$$+ \frac{2x_{12}}{R}\frac{\partial u_1}{\partial x}\left(\frac{\partial u_2}{\partial \theta} + u_3\right) + x_{66}\left(\frac{\partial u_2}{\partial x} + \frac{1}{R}\frac{\partial u_1}{\partial \theta}\right)^2$$
$$- 2y_{11}\left(\frac{\partial u_1}{\partial x}\right)\left(\frac{\partial^2 u_3}{\partial x^2}\right) - \frac{2y_{12}}{R^2}\left(\frac{\partial u_1}{\partial x}\right)\left(\frac{\partial^2 u_3}{\partial \theta^2} - \frac{\partial u_2}{\partial \theta}\right)$$
$$- \frac{2y_{12}}{R}\left(\frac{\partial u_2}{\partial \theta} + u_3\right)\left(\frac{\partial^2 u_3}{\partial x^2}\right)$$
$$- \frac{2y_{22}}{R^3}\left(\frac{\partial u_2}{\partial \theta} + u_3\right)\left(\frac{\partial^2 u_3}{\partial \theta^2} - \frac{\partial u_2}{\partial \theta}\right)$$
$$- \frac{4y_{66}}{R}\left(\frac{\partial u_2}{\partial x} + \frac{1}{R}\frac{\partial u_1}{\partial \theta}\right)\left(\frac{\partial^2 u_3}{\partial x \partial \theta} - \frac{3}{4}\frac{\partial u_2}{\partial x} + \frac{1}{4R}\frac{\partial u_1}{\partial \theta}\right)$$
$$+ z_{11}\left(\frac{\partial^2 u_3}{\partial x^2}\right)^2 + \frac{z_{22}}{R^4}\left(\frac{\partial^2 u_3}{\partial \theta^2} - \frac{\partial u_2}{\partial \theta}\right)^2$$
$$+ \frac{2z_{12}}{R^2}\left(\frac{\partial^2 u_3}{\partial x^2}\right)\left(\frac{\partial^2 u_3}{\partial \theta^2} - \frac{\partial u_2}{\partial \theta}\right)$$
$$\left. + \frac{4z_{66}}{R^2}\left(\frac{\partial^2 u_3}{\partial x \partial \theta} - \frac{3}{4}\frac{\partial u_2}{\partial x} + \frac{1}{4R}\frac{\partial u_1}{\partial \theta}\right)^2\right] dx d\theta$$

The kinetic energy T for a CS is expressed as:

$$T = \frac{1}{2}\int_0^L \int_0^{2\pi} \rho_t \left[\left(\frac{\partial u_1}{\partial t}\right)^2 \quad (10)\right.$$
$$\left. + \left(\frac{\partial u_2}{\partial t}\right)^2 + \left(\frac{\partial u_3}{\partial t}\right)^2\right] R d\theta dx$$

here time variable is denoted by t and the mass density per unit length is represented by ρ_t and is written as:

$$\rho_t = \int_{-H/2}^{H/2} \rho dz \quad (11)$$

where ρ is mass density.
The Lagrange energy functional Γ for a CS is defined as a function of the kinetic and strain energies as:

$$\Gamma = T - \Im \quad (12)$$

3 Numerical Procedure

The present cylindrical shell is solved by the Rayleigh-Ritz technique. Its deformation displacement fields are expressed in terms of product of functions of space and time variables. These functions for a CS with ring supports can be assumed in the longitudinal, tangential and transverse directions as:

$$u_1(x,\theta,t) = a_m U(x)\cos n\theta \sin\omega t \quad (13)$$
$$u_2(x,\theta,t) = b_m V(x)\sin n\theta \sin\omega t$$
$$u_3(x,\theta,t) = c_m W(x)\cos n\theta \sin\omega t$$

here $U(x) = \frac{d\overline{\xi}(x)}{dx}$, $V(x) = \overline{\xi}(x)$, and $W(x) = \overline{\xi}(x)\prod_{i=1}^{P}(x-a_i)^{\ell_i}$ and $\overline{\xi}(x)$ signifies the axial function that fulfills end point conditions. In the longitudinal direction at $x = a_i$, i^{th}ring support is present. Here $\ell_i = 1$ and $\ell_i = 0$ represents with and without a ring support respectively. n is the circumferential wave number and ω is the angular vibration frequency. The coefficients a_m, b_m and c_m signify the vibration's amplitudes in the x, θ and z directions respectively and m is the axial half wave number in the axial direction.$\overline{\xi}(x)$is chosen for the axial deformation function which is the characteristic beam function as in reference [10]:

$$\overline{\xi}(x) = \beta_1\cosh(\alpha_m x) + \beta_2\cos(\alpha_m x) - \chi_m(\beta_3\sinh(\alpha_m x) + \beta_4\sin(\alpha_m x)) \quad (14)$$

where the values of β_i , $(i = 1,2,3,4)$,depend upon the nature of the edge conditions and α_m denotes the roots of trigonometric or hyperbolic equations and the parameters, $\chi_m{}'s$ depend on values of α_m.
Following dimensionless parameters are utilized to simplify the problem.

$$\underline{U} = \frac{U(x)}{H},\ \underline{V} = \frac{V(x)}{H},\ \underline{W} = \frac{W(x)}{R} \quad (15)$$
$$\underline{x}_{ij} = \frac{x_{ij}}{H},\ \underline{y}_{ij} = \frac{y_{ij}}{H^2},\ \underline{z}_{ij} = \frac{z_{ij}}{H^3}$$
$$\alpha = R/L,\ \beta = H/R,\ X = \frac{x}{L},\ \underline{\rho}_t = \frac{\rho_t}{H}$$

Now the expressions (13) are re-written as:

$$u_1(x,\theta,t) = a_m H\underline{U}\cos n\theta\sin\omega t \quad (16)$$
$$u_2(x,\theta,t) = b_m H\underline{V}\sin n\theta\sin\omega t$$
$$u_3(x,\theta,t) = c_m R\underline{W}\cos n\theta\sin\omega t$$

After making substitutions of the expressions (16) and their respective derivatives into the relations (9) and (10), $\Im_{\max}$ and $T_{\max}$ are obtained using the principle of conservation of energy. By applying the principle of maximum energy, the Lagrange functional, $\Gamma_{\max}$ takes the following form:

$$\Gamma_{\max} = \frac{\pi HLR}{2}\Bigg[R^2\omega^2\underline{\rho}_t\int_0^1\left(\beta^2(a_m\underline{U})^2 + \beta^2(b_m\underline{V})^2 + (c_m\underline{W})^2\right)dX - \int_0^1\Bigg\{\alpha^2\beta^2\underline{x}_{11}\left(a_m\frac{d\underline{U}}{dX}\right)^2 + \underline{x}_{22}(-n\beta b_m\underline{V} + c_m\underline{W})^2 + 2\alpha\beta\underline{x}_{12}\left(a_m\frac{d\underline{U}}{dX}\right) \times(-n\beta b_m\underline{V} + c_m\underline{W}) + \underline{x}_{66}\left(\alpha\beta b_m\frac{d\underline{V}}{dX} + n\beta a_m\underline{U}\right)^2 - 2\alpha^3\beta^2\underline{y}_{11}\left(a_m\frac{d\underline{U}}{dX}\right)\left(c_m^2\frac{d^2\underline{W}}{dX^2}\right) - 2\alpha\beta^2\underline{y}_{12} \times\left(a_m\frac{d\underline{U}}{dX}\right)\left(-n^2c_m\underline{W} + n\beta b_m\underline{V}\right) - 2\alpha^2\beta\underline{y}_{12} \times(-n\beta b_m\underline{V} + c_m\underline{W})\left(c_m^2\frac{d^2\underline{W}}{dX^2}\right) - 2\beta\underline{y}_{22}(-n\beta b_m\underline{V} + c_m\underline{W})\left(-n^2c_m\underline{W} + n\beta b_m\underline{V}\right) - 4\beta\underline{y}_{66}\left(\alpha\beta b_m\frac{d\underline{V}}{dX} + n\beta a_m\underline{U}\right) \cdot\left(n\alpha c_m\frac{d\underline{W}}{dX} - \frac{3\alpha\beta}{4}b_m\frac{d\underline{V}}{dX} + \frac{n\beta}{4}a_m\underline{U}\right) + \alpha^4\beta^2\underline{z}_{11}\left(c_m^2\frac{d^2\underline{W}}{dX^2}\right)^2 + \beta^2\underline{z}_{22}\left(-n^2c_m\underline{W} + n\beta b_m\underline{V}\right)^2 + 2\alpha^2\beta^2\underline{z}_{12}\left(c_m^2\frac{d^2\underline{W}}{dX^2}\right)\times\left(-n^2c_m\underline{W} + n\beta b_m\underline{V}\right) + 4\underline{z}_{66}\left(n\alpha c_m\frac{d\underline{W}}{dX} - \frac{3\alpha\beta}{4}b_m\frac{d\underline{V}}{dX} + \frac{n\beta}{4}a_m\underline{U}\right)^2\Bigg\}dX\Bigg] \quad (17)$$

4 Formation of eigenvalue frequency equation

The shell eigenvalue frequency equation is derived by making a use of the Rayleigh-Ritz technique. The energy Lagrange functional $\Gamma_{\max}$ is extremized with regard to vibration coefficients: a_m, b_m and c_m, we obtain the following relations.

$$\frac{\partial\Gamma_{\max}}{\partial a_m} = \frac{\partial\Gamma_{\max}}{\partial b_m} = \frac{\partial\Gamma_{\max}}{\partial c_m} = 0 \quad (18)$$

A system of homogeneous simultaneous equations in a_m, b_m and c_m is generated and is transformed into the eigenvalue problem as.

$$\left\{[K] - \Omega^2[M]\right\}\overline{X} = 0 \quad (19)$$

where $[K]$ is the stiffness matrix and $[M]$represents the mass matrix and

$$\Omega^2 = R^2\omega^2\underline{\rho}_t \tag{20}$$

and

$$\overline{X}' = [a_m,\ b_m,\ c_m] \tag{21}$$

The elements of $[K]$ and $[M]$ are given in the Appendix 1. MATLAB software is used to solve the eigenvalue problem (19) for the shell frequency spectra for various physical parameters.

5 Functionally graded materials

In practice of three layered cylindrical shell, its central layer is fabricated by FGMs and isotropic is used for internal and external layers as shown in Figure 2. Here the stiffness moduli are altered as:

$$\begin{aligned} x_{ij} &= x_{ij}^{int(I)} + x_{ij}^{cen(F)} + x_{ij}^{ext(I)} \\ y_{ij} &= y_{ij}^{int(I)} + y_{ij}^{cen(F)} + y_{ij}^{ext(I)} \\ z_{ij} &= z_{ij}^{int(I)} + z_{ij}^{cen(F)} + z_{ij}^{ext(I)} \end{aligned} \tag{22}$$

where *i,j*=1, 2, 6 and superscript $int(I)$, $ext(I)$ represent the isotropic internal and external layers and $cen(F)$ denotes the central FGM layer. The functionally graded materials contain two essential materials. These materials are stainless steel and nickel. The material parameters for stainless steel material are: E_2, μ_2, ρ_2 and for nickel material are: E_1, μ_1, ρ_1. The thickness of each layer is presumed to be $H/3$. Then the actual material quantities for FGM layer are given as:

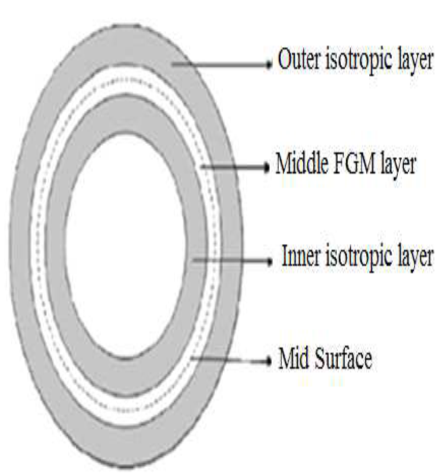

Figure 2: Cross-section of three-layered CS.

$$E_F = [E_1 - E_2]\left(\frac{6z+H}{2H}\right)^N + E_2 \tag{23a}$$

$$\mu_F = [\mu_1 - \mu_2]\left(\frac{6z+H}{2H}\right)^N + \mu_2 \tag{23b}$$

$$\rho_F = [\rho_1 - \rho_2]\left(\frac{6z+H}{2H}\right)^N + \rho_2 \tag{23c}$$

The material properties for middle FGM layer vary from $z = -H/6$ to $H/6$. From the relations (23a-c), the effective material properties become $E_F = E_2$, $\mu_F = \mu_2$ and $\rho_F = \rho_2$ at $z = -H/6$ where for $z = H/6$ material properties become$E_F = E_1$, $\mu_F = \mu_1$ and $\rho_F = \rho_1$. Thus for$z = -H/6$, the shell is contained only stainless steel whereas for $z = H/6$ consisted of nickel material. In a FGM shell, the distribution of materials is controlled by various volume fraction laws. Three volume fraction laws are expressed in mathematical form. If z symbolizes the basic shell thickness variable then the volume fraction law V_F of a FGM is formulated as following function [24]

$$V_F = \left(\frac{6z+H}{2H}\right)^N \tag{24}$$

where H represents the thickness of cylinder-shaped shell and N denotes the power law proponent which may take values from zero to infinity. A volume fraction law formulated by Arshad *et al.* [14] as:

$$V_F = 1 - e^{-\left(\frac{6z+H}{2H}\right)^N} \tag{25}$$

where e be the standard irrational natural exponential base number. The material properties are written as:

$$E_F = [E_1 - E_2]\left[1 - e^{-\left(\frac{6z+H}{2H}\right)^N}\right] + E_2 \tag{25a}$$

$$\mu_F = [\mu_1 - \mu_2]\left[1 - e^{-\left(\frac{6z+H}{2H}\right)^N}\right] + \mu_2 \tag{25b}$$

$$\rho_F = [\rho_1 - \rho_2]\left[1 - e^{-\left(\frac{6z+H}{2H}\right)^N}\right] + \rho_2 \tag{25c}$$

Trigonometric volume fraction law for a FGM circular CS is stated as:

$$\begin{aligned} V_{F_1} &= \sin^2\left[\left(\frac{6z+H}{2H}\right)^N\right], \\ V_{F_2} &= \cos^2\left[\left(\frac{6z+H}{2H}\right)^N\right] \end{aligned} \tag{26}$$

Table 1: Comparison of frequency parameter $\Delta = \omega R\sqrt{(1-\mu^2)\rho/E}$ for simply-supported isotropic CS. ($\mu = 0.3, m = 1, H/R = 0.05$)

L/R		n	n	n	n
		1	2	3	4
20	Zhang *et al.*[18]	0.016102	0.039271	0.109811	0.210277
20	Present	0.0161029	0.0392713	0.1098115	0.2102771
20	Difference %	0.006	0.001	0.001	0.000

Table 2: Comparison of frequency parameter $\Delta = \omega R\sqrt{(1-\mu^2)\rho/E}$ for a clamped isotropic shell ($\mu = 0.3, H/R = 0.05$)

L/R		n	n	n	n
		1	2	3	4
20	Zhang *et al.*[18]	0.03285	0.040638	0.109973	0.210324
20	Present	0.03440	0.040772	0.110005	0.210376
20	Difference %	4.7	0.33	0.03	0.02

Table 3: Comparison of natural frequencies (Hz) for type I FGM cylindrical shell with simply supported edges. ($m = 1, H/R = 0.002, L/R = 20$)

	Loy *et al.* [1]			Present		
		N			N	
n	0.5	1	2	0.5	1	2
1	13.321	13.211	13.103	13.321	13.210	13.103
2	4.5168	4.4800	4.4435	4.5098	4.4746	4.4396
3	4.1911	4.1569	4.1235	4.1520	4.1356	4.1154
4	7.0972	7.0384	6.9820	7.0189	7.0000	6.9721
5	11.336	11.241	11.151	11.210	11.181	11.138

Here

$$V_{F1} + V_{F2} = 1 \tag{26a}$$

The material parameters for FG cylindrical shell are written as:

$$E_F = [E_1 - E_2]\sin^2\left[\left(\frac{6z+H}{2H}\right)^N\right] + E_2 \tag{26b}$$

$$\mu_F = [\mu_1 - \mu_2]\sin^2\left[\left(\frac{6z+H}{2H}\right)^N\right] + \mu_2 \tag{26c}$$

$$\rho_F = [\rho_1 - \rho_2]\sin^2\left[\left(\frac{6z+H}{2H}\right)^N\right] + \rho_2 \tag{26d}$$

6 Results and discussion

To check the validity of the current work, results for simply supported and clamped CSs with no ring support are compared with others available in the literature. A good agreement is found among the present results and those obtained by other techniques. In Table 1, a comparison of frequency parameters $\Delta = \omega R\sqrt{(1-\mu^2)\rho/E}$ for simply supported isotropic CS is presented with those in Zhang *et al.* [18]. Table 3 represents the NFs (Hz) for a simply supported FGM cylindrical shell of type 1 compared with those obtained by Loy *et al.* [1] and for power law exponents N = 0.5, 1, 2. The frequency at $n = 3$ which is about 0.9%, 0.5%, and 0.1% minimum than those available in [1]. It is determined from the comparison of NFs that the current method is efficient and gives accurate results. Two types of CS are described in Table 4. where M_A, M_B and M_C represent Aluminum, Stainless Steel and Nickel respectively. Material properties of the isotropic material as well as FGM constituents are given in reference [1] and [2]. Different layer thicknesses were used for the analysis of three-layered FGM cylindrical shell as shown in Table 5.

Table 6-8 show the variation of NFs (Hz) versus n for three layered FGMs type I CS with ring supports. Thickness of the center layer is presumed to be *H/3*, *H/2* and *3H/5*

Table 4: Types of shell w. r. t the arrangements of shell layers

Types	Internal Layer	Central FGM Layer	External Layer
Type I	M_A	M_B/M_C	M_A
Type II	M_A	M_C/M_B	M_A

Table 5: Thickness variation of the FGM shell layers

Thickness Patterns	Inner isotropic Layer	Central FGM Layer	External isotropic Layer
Case 1	$H/3$	$H/3$	$H/3$
Case 2	$H/4$	$H/2$	$H/4$
Case 3	$H/5$	$3H/5$	$H/5$

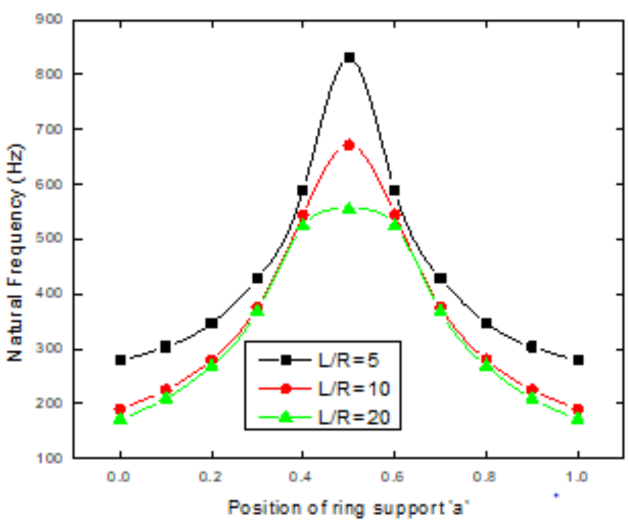

Figure 3: Variation of NFs (Hz) of three-layered FGM CS versus ring supports position 'a' at different L/R ratios for $SS-SS$ edge conditions. ($m = 1$, $n = 1$, $H/R = 0.005$ and $N = 2$)

for Tables 6-8 respectively. In these Tables, the influence of three VFL is perceived for six edge conditions: simply supported-simply supported ($SS-SS$), clamped-clamped ($C-C$), free-free ($F-F$), clamped-simply supported ($C-SS$), clamped-free ($C-F$) and free-simply supported ($F-SS$).It is noticed that the NF increased with the increase of n. It is also examined that the $C-C$ edge condition has the maximum NFs (Hz) and $C-F$ has the really minimum. It is studied that natural frequencies increasing swiftly from n is equal to 1 to 2 then its increasing steadily. In Table 6, Law-I gets the extreme frequencies (Hz) and Law-III takes the lowest frequencies (Hz). Table 7 & 8 represent the variation of NFs (Hz) of FGM shell by using Law-I for six boundary conditions.

Table 9-11 describe the variation of NFs (Hz), effects of shell configurations on NFs (Hz) versus n for FGM shell type II with ring supports. Thickness of the center layer is supposed as same as for Table 6, 7 and 8 respectively. Law-I gets the lowest values and Law-III takes extreme values of NFs (Hz) in Table 9.

Table 12 represents the natural frequency (Hz) of three layered CS of case1 versus n with and without ring support for $SS-SS$ boundary conditions. The behavior of frequency remains same according to the circumferential wave number n and volume fraction laws for both CSs with and without ring support. Table 12 shows that the NFs of CS with ring support are higher than frequencies of the CS without ring support.

Table 13 demonstrates NFs (Hz) with ratios (L/R) for type I & case 1 FGM shell. The natural frequencies decreased less than 0.5% with the increasing values of N. Natural frequencies decreased 11% and 14% when L/R becomes 10 and 20 respectively.

The thickness of each layer of the shell for Figure 3-8 is $H/3$. Natural frequency varies with respect to the ring support position and this influence changes according to edge conditions. Figure 3 shows the variation of NF of $SS-SS$ shell with the position of 'a' for different L/R ratios. Natural frequencies are obtained for law-I, law-II and law-III. The movements of these VFL, for frequency curve at $a = 0$, the values are 328.96 , 328.51, 327.88, at $a = 0.5$, the values are 593.99, 593.17, 592.85 and at $a = 1$,values are 328.97, 328.51, 327.89 for law-I, law-II and law-III respectively. The behavior of the frequency curve is increasing from $a = 0$ to $a = 0.5$ and decreasing from $a = 0.5$ to $a = 1$. So it is a symmetric curve. Similar behavior studied for L/R =10, 20 and also for $C-C$ and $F-F$ edge conditions. Moreover, law-II is consisted between the law-I & III. Frequency curves are overlapping because the values for all laws are so closed to each other. So for other boundary conditions law-III is selected to draw because it attains minimum frequency values. Figure 4 shows the same results for clamped-clamped edge condition. Frequencies are significantly high for clamped-clamped end condition. In Figure 5 variation of NFs (Hz) of three-layered FGM cylindrical shell is plotted against the ring supports position. So the frequency value at $a = 0$, is 260.46 and the extreme NF (Hz) for law-III lies at $a = 0.6$, frequency is 683.25. The last value of frequency curve is 278.24 lies at $a = 1$,. Similar behavior displays for $L/R = 10$ and 20. In Figure 6. The frequency curve is increasing gradually from $a = 0$ to 0.5 then gets its extreme value at $a = 0.8$, after this curve starts to decrease. Here the frequency curve is not chime formed because of different edge condition. It is noticed that the behavior of NFs curves for all ratios and laws are same. Fig-

Table 6: Variation of NFs (Hz) for Type I & Case 1 FGM CS against n with ring support. ($L/R = 50$, $m = 1$, $H/R = 0.007$, $a = 0.5$, $N = 1$)

	n	$SS-SS$	$C-C$	$F-F$	$C-SS$	$C-F$	$F-SS$
Law I	1	505.393	513.611	503.363	507.878	278.876	503.485
	2	848.181	848.183	48.182	762.667	349.123	817.553
	3	848.297	848.3	48.299	773.636	367.637	822.354
	4	848.604	848.61	848.608	777.258	375.168	823.97
	5	849.247	849.256	849.253	779.396	379.799	825.189
	6	850.411	850.424	850.42	781.42	384.072	826.677
	7	852.321	852.338	852.333	783.941	389.226	828.811
	8	855.239	855.261	855.254	787.392	396.115	831.918
	9	859.46	859.488	859.479	792.16	405.447	836.328
	10	865.311	865.346	865.335	798.631	417.851	842.389
Law II	1	504.242	512.441	502.216	506.72	278.238	502.338
	2	846.248	846.25	846.249	760.929	348.327	815.69
	3	846.377	846.38	846.379	771.884	366.804	820.492
	4	846.701	846.706	846.705	775.514	374.326	822.122
	5	847.366	847.374	847.372	777.669	378.96	823.36
	6	848.556	848.569	848.565	779.715	383.24	824.874
	7	850.497	850.514	850.509	782.264	388.404	827.038
	8	853.45	853.472	853.465	785.747	395.305	830.179
	9	857.711	857.739	857.73	790.55	404.65	834.627
	10	863.605	863.64	863.629	797.06	417.066	840.73
Law III	1	503.416	511.602	501.394	505.891	277.779	501.515
	2	844.84	844.841	844.841	759.663	347.748	814.332
	3	844.949	844.952	844.951	770.583	366.186	819.108
	4	845.246	845.252	845.25	774.182	373.684	820.709
	5	845.875	845.884	845.881	776.302	378.294	821.913
	6	847.022	847.035	847.031	778.307	382.549	823.383
	7	848.911	848.928	848.922	780.806	387.683	825.495
	8	851.802	851.825	851.817	784.231	394.548	828.577
	9	855.993	856.021	856.012	788.969	403.85	832.956
	10	861.808	861.843	861.831	795.404	416.218	838.981

Table 7: Variation of NFs (Hz) for Type I & Case 2 FGM CS against *n* with ring support. ($L/R = 50$, $m = 1$, $H/R = 0.007$, $a = 0.5$, $N = 1$)

n	$SS-SS$	$C-C$	$F-F$	$C-SS$	$C-F$	$F-SS$
1	499.678	507.874	497.709	502.171	276.964	497.805
2	842.358	842.36	842.359	757.432	346.726	811.926
3	842.477	842.481	842.48	768.329	365.114	816.711
4	842.788	842.793	842.792	771.93	372.594	818.322
5	843.433	843.441	843.438	774.059	377.193	819.538
6	844.595	844.608	844.603	776.074	381.434	821.022
7	846.498	846.515	846.509	778.583	386.546	823.147
8	849.4	849.422	849.415	782.012	393.376	826.237
9	853.595	853.623	853.613	786.748	402.625	830.619
10	859.406	859.44	859.428	793.172	414.918	836.637

Table 8: Variation of NFs (Hz) for Type I & Case 3 FGM CS against *n* with ring support. ($L/R = 50$, $m = 1$, $H/R = 0.007$, $a = 0.5$, $N = 1$)

n	$SS-SS$	$C-C$	$F-F$	$C-SS$	$C-F$	$F-SS$
1	496.300	504.482	494.366	498.797	275.838	494.447
2	838.929	838.931	838.930	754.349	345.315	808.612
3	839.052	839.055	839.054	765.205	363.630	813.389
4	839.367	839.372	839.371	768.797	371.083	815.000
5	840.017	840.026	840.023	770.925	375.671	816.220
6	841.186	841.199	841.195	772.943	379.906	817.709
7	843.096	843.113	843.108	775.456	385.014	819.840
8	846.006	846.028	846.021	778.891	391.839	822.937
9	850.209	850.236	850.227	783.633	401.082	827.326
10	856.027	856.061	856.050	790.062	413.365	833.350

Table 9: Variation of NFs (Hz) for Type II & Case 1 FGM CS against *n* with ring support. ($L/R = 50$, $m = 1$, $H/R = 0.007$, $a = 0.5$, $N = 1$)

	n	$SS-SS$	$C-C$	$F-F$	$C-SS$	$C-F$	$F-SS$
Law I	1	505.880	514.077	503.833	508.352	278.623	503.965
	2	847.410	847.411	847.411	761.974	348.805	816.815
	3	847.519	847.522	847.521	772.927	367.301	821.601
	4	847.817	847.823	847.821	776.537	374.822	823.206
	5	848.448	848.457	848.455	778.664	379.448	824.413
	6	849.598	849.612	849.608	780.676	383.719	825.889
	7	851.492	851.513	851.508	783.185	388.875	828.010
	8	854.393	854.422	854.415	786.624	395.770	831.104
	9	858.598	858.636	858.628	791.383	405.114	835.503
	10	864.433	864.483	864.473	797.847	417.537	841.553
Law II	1	507.040	515.256	504.988	509.517	279.264	505.120
	2	849.352	849.353	849.353	763.720	349.605	818.687
	3	849.448	849.452	849.451	774.687	368.137	823.471
	4	849.729	849.735	849.733	778.289	375.667	825.063
	5	850.339	850.348	850.345	780.399	380.291	826.250
	6	851.463	851.477	851.472	782.388	384.555	827.701
	7	853.329	853.346	853.341	784.870	389.701	829.792
	8	856.197	856.220	856.213	788.277	396.584	832.852
	9	860.367	860.395	860.386	793.000	405.916	837.212
	10	866.165	866.199	866.188	799.426	418.327	843.222
Law III	1	507.880	516.109	505.824	510.361	279.730	505.956
	2	850.780	850.782	850.781	765.004	350.192	820.064
	3	850.896	850.899	850.898	776.006	368.763	824.874
	4	851.204	851.210	851.208	779.639	376.318	826.495
	5	851.849	851.858	851.855	781.785	380.965	827.717
	6	853.018	853.030	853.026	783.815	385.255	829.211
	7	854.935	854.953	854.947	786.347	390.431	831.354
	8	857.865	857.887	857.880	789.812	397.350	834.474
	9	862.105	862.133	862.124	794.601	406.725	838.903
	10	867.982	868.017	868.006	801.101	419.185	844.991

Table 10: Variation of NFs (Hz) for Type II & Case 2 FGM CS against *n* with ring support. ($L/R = 50$, $m = 1$, $H/R = 0.007$, $a = 0.5$, $N = 1$) .

n	$SS-SS$	$C-C$	$F-F$	$C-SS$	$C-F$	$F-SS$
1	500.409	508.573	498.414	502.883	276.586	498.525
2	841.206	841.208	841.207	756.396	346.253	810.824
3	841.310	841.313	841.312	767.265	364.611	815.580
4	841.600	841.606	841.604	770.843	372.076	817.169
5	842.221	842.230	842.227	772.949	376.667	818.362
6	843.356	843.369	843.365	774.940	380.907	819.820
7	845.231	845.248	845.243	777.424	386.029	821.918
8	848.107	848.129	848.122	780.833	392.880	824.983
9	852.279	852.307	852.298	785.553	402.168	829.344
10	858.073	858.108	858.096	791.967	414.518	835.348

Table 11: Variation of NFs (Hz) for Type II & Case 3 FGM CS against *n* with ring support.($L/R = 50$, $m = 1$, $H/R = 0.007$, $a = 0.5$, $N = 1$).

n	$SS-SS$	$C-C$	$F-F$	$C-SS$	$C-F$	$F-SS$
1	497.177	505.321	495.213	499.652	275.387	495.311
2	837.550	837.551	837.551	753.109	344.748	807.294
3	837.650	837.653	837.652	763.926	363.024	812.031
4	837.933	837.938	837.936	767.484	370.452	813.608
5	838.542	838.551	838.548	769.572	375.016	814.787
6	839.661	839.674	839.670	771.543	379.227	816.227
7	841.513	841.530	841.524	774.002	384.310	818.302
8	844.356	844.378	844.371	777.376	391.108	821.334
9	848.485	848.513	848.504	782.050	400.323	825.651
10	854.223	854.257	854.246	788.406	412.578	831.597

Table 12: Variation of NFs (Hz) of three layered FGM CS Type I & Case1 versus circumferential wave number (*n*). ($L/R = 50$, $m = 1$, $H/R = 0.007$, $a = 0.5$, $N = 1$).

	without ring support	with ring support
n	Type I	Type I
1	1.6289	505.393
2	4.6222	848.181
3	12.991	848.297
4	24.903	848.604
5	40.271	849.247
6	59.076	850.411
7	81.309	852.321
8	106.968	855.239
9	136.052	859.460
10	168.559	865.311

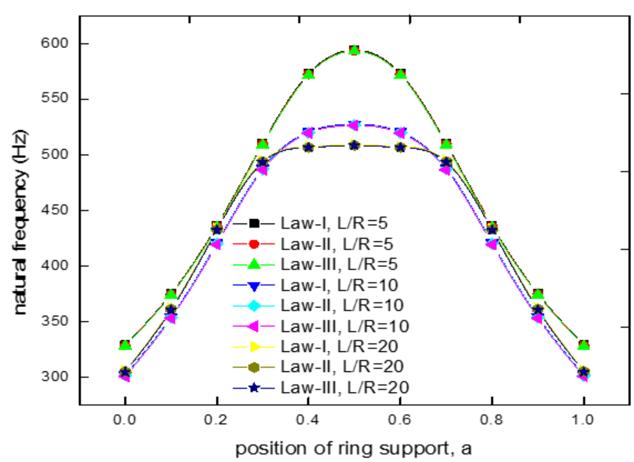

Figure 4: Variation of NFs (Hz) of three-layered FGM CS with ring supports position '*a*' at different L /R ratios for Law-I, $C-C$ edge conditions. ($m = 1$, $n = 1$, $H/R = 0.005$ and $N = 2$)

ures 7 and 8 exhibits variation of NFs (Hz) versus *n* for different *N* with $a = 0.5$ for $SS-SS$ and $C-C$ end point conditions. Here *N* differs as 0.5, 1 and 2. Here frequency curves increase rapidly from $n = 1$ to 2 and then these curves start to increase linearly through *n*. It is noticed that with the increase in power law exponent *N* natural frequency is not really affected.

Table 13: Natural Frequencies (Hz) of Type I & Case 1 FGM CS with ring support versus length to radius ratios L/R. ($n = 1, m = 1, , H/R = 0.005, a = 0.5$).

L/R	N=1	N=2	N=3	N=4	N=5	N=10	N=20	N=30	N=50
5	595.701	593.988	593.135	592.625	592.285	591.513	591.067	590.905	590.763
10	528.705	527.184	526.427	525.973	525.672	524.985	524.587	524.440	524.309
20	510.584	509.115	508.384	507.946	507.655	506.991	506.607	506.464	506.337

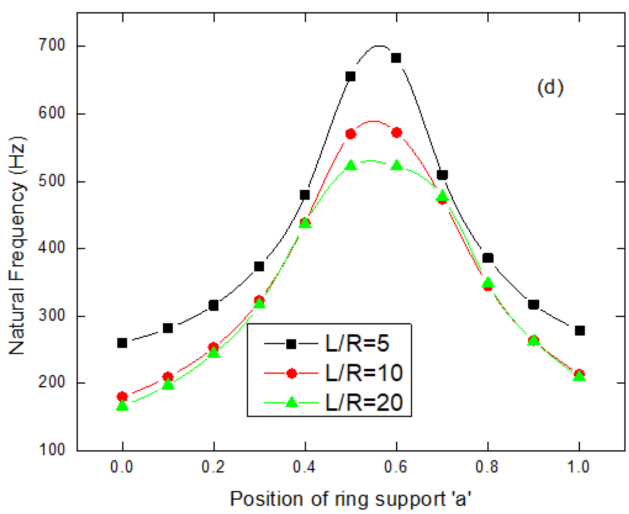

Figure 5: Variation of NFs (Hz) of three-layered FGM CS versus ring supports position 'a' at different L/R ratios for C–SS edge conditions. ($m = 1, n = 1, H/R = 0.005$ and $N = 2$)

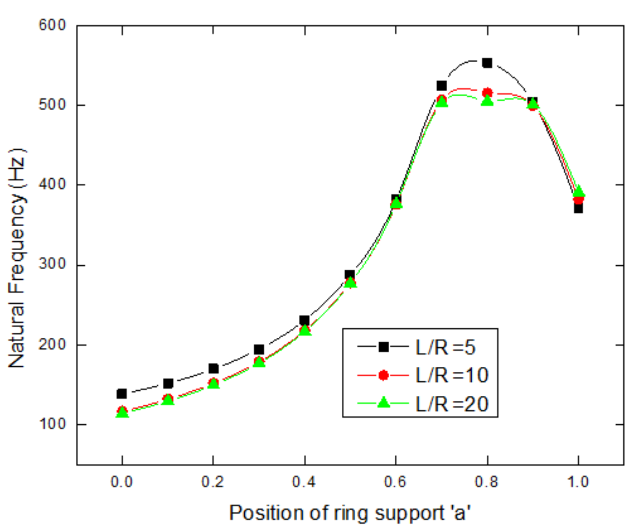

Figure 6: Variation of NFs (Hz) of three-layered FGM CS versus ring supports position 'a' at different L/R ratios for $C - F$ edge conditions. ($m = 1, n = 1, H/R = 0.005$ and $N = 2$)

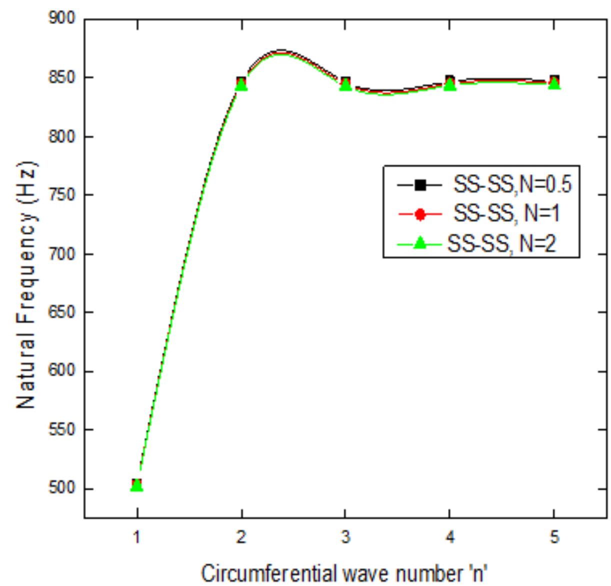

Figure 7: Variation of NFs (Hz) of FGM cylindrical shell versus (n) for different N with $SS - SS$ edge conditions. (m=1, L/R=50, H/R=0.007)

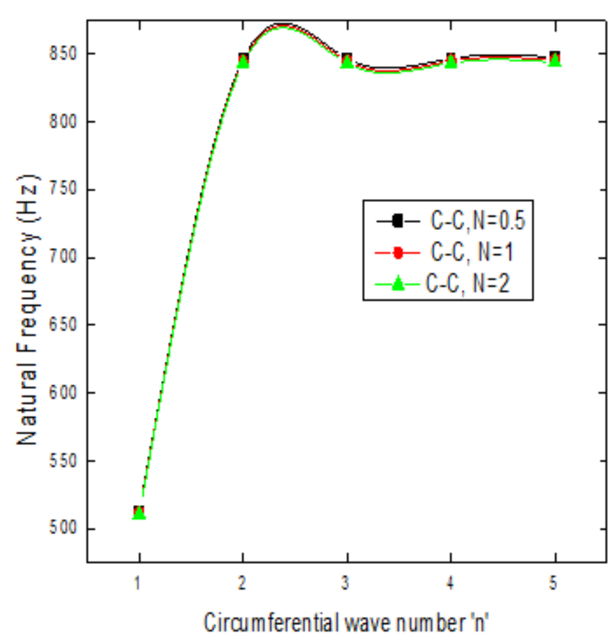

Figure 8: Variation of NFs (Hz) of FGM cylindrical shell versus (n) for different N with $C - C$ edge conditions. (m=1, L/R=50, H/R=0.007)

7 Conclusions

The frequency analysis of three-layered FGM cylindrical shell is performed to determine the effect of ring support. The shell central layer is made of FGMs while the internal and external layers are of isotropic material. Variation of NFs (Hz) is analyzed for six boundary conditions. It is concluded that the material dissemination controlled by the VFL which has little effect (<1%) on vibration frequency of a FGM CS but law-III is recommended for type 1 FGM shell and law-I is for type 2 FGM shell to estimate the lower frequency values.

Natural frequencies are increased with the increase of n and decreased with the increase of L/R ratios. Natural frequency also decreased <2% when increase in the thickness of the central layer becomes double. The frequency curve of the shell with ring support at different positions get symmetric shapes because of same edge conditions. They are not symmetrical about center because of different end point conditions. The induction of ring support on cylinder-shaped shell has significant effect on the NFs as compared to the shell frequencies without ring support.

References

[1] Loy C. T., Lam K.Y., and Reddy J.N., Vibration of functionally graded cylindrical shells, Int. J. Mech. Sci., 1999, 41, 309-324.
[2] Pradhan S.C., Loy, C.T., Lam K.Y., and Reddy J.N., Vibration characteristics of functionally graded cylindrical shells under various boundary conditions. Appl. Acoust., 2000, 61, 111-129.
[3] Chen W.Q., Bian Z.G., and Ding H.J., Three-dimensional vibration analysis of fluid-filled orthotropic FGM cylindrical shells, Int. J. Mech. Sci., 2004, 46, 159-171.
[4] Zhi-Yuan C., and Hua-Ning W., Free vibration of FGM cylindrical shells with holes under various boundary conditions, J. Sound Vib. 2007, 306, 227-237.
[5] Haddadpour H., Mahmoudkhani S., and Navazi H.M., Free vibration analysis of functionally graded cylindrical shells including thermal effects, Thin-Walled Structures, 2007, 45, 591-599.
[6] Iqbal Z., Naeem, M.N., and Sultana, N., Vibration characteristics of FGM circular cylindrical shells using wave propagation approach, Acta Mech., 2009, 208, 237-248.
[7] Iqbal Z., Naeem, M.N., Sultana, N., Arshad, S.H., and Shah, A.G., Vibration characteristics of FGM circular cylindrical shells filled with fluid using wave propagation approach, Appl. Math. Mech.,2009, 30, 1393-1404.
[8] Niino M., Hirai T., and Watanabe R., The functionally gradient materials, J. Jap. Soc. Comp. Mater, 1987, 13, 257-264.
[9] Lam, K.Y., and Loy, C.T., Effects of boundary conditions on frequencies of a multi-layered cylindrical shell, J. Sound Vib., 1995, 188, 363-384.
[10] Loy, C.T., and Lam, K.Y., Vibration of cylindrical shells with ring support, Int. J. Mech. Sci., 1997, 39, 455-471.
[11] Xiang, Y., Ma, Y.F., Kitipornchai, S., Lim, C.W., and Lau, C.W.H., Exact solutions for vibration of cylindrical shells with intermediate ring supports, Int. J. Mech. Sci., 2002, 44, 1907-1924.
[12] Zhang L., and Xiang Y., Vibration of open circular cylindrical shells with intermediate ring supports, Int. J. Solids Struct., 2006, 43, 3705-3722.
[13] Swaddiwudhipong, S., Tian, J., and Wang, C. M., Vibrations of cylindrical shells with intermediate supports, J. Sound Vib., 1995, 187, 69-93.
[14] Arshad S.H., Naeem M.N., and Sultana N., Frequency analysis of functionally graded cylindrical shells with various volume fraction laws, J. Mech. Eng. Sci., 2007, 221, 1483-1495.
[15] Arshad S.H., Naeem M.N., Sultana N., Shah,A.G., and Iqbal Z., Vibration analysis of bi-layered FGM cylindrical shells, Arch. Appl. Mech., 2011, 81, 319-343.
[16] Sofiyev A.H., and Avcar, M., The stability of cylindrical shells containing an FGM layer subjected to axial load on the Pasternak foundation, Engineering, 2010, 2, 228-236.
[17] Arshad S.H., Naeem M.N., Sultana N., Iqbal Z., and Shah A.G., Vibration of bi-layered cylindrical shells with layers of different materials, J. Mech. Sci. Tech, 2010, 24, 805-810.
[18] Zhang L., Xiang Y., and Wei G.W., Local adaptive differential quadrature for free vibration analysis of cylindrical shells with various boundary conditions, Int. J. Mech. Sci., 2006, 48, 1126-1138.
[19] Naeem M.N., Khan A.G., Arshad S.H., Shah A.G., and Gamkhar M., Vibration of three-layered FGM cylindrical shells with middle layer of isotropic material for various boundary conditions, World J. Mech., 2014, 4, 315-331.
[20] Arshad S.H., Naeem M.N., and Soutis, C., Influence of ring support on free vibration of sandwich functionally graded cylindrical shells with middle layer of isotropic material, J. Eng. Res., 2016, 4, 159-186.
[21] Li S.R., Fu X.H., and Batra R.C., Free vibration of three-layer circular cylindrical shells with functionally graded middle layer, Mech. Res. Commun., 2010, 37, 577-580.
[22] Ghamkhar M., Naeem, M.N., Imran M., Kamran M., and Soutis, C., Vibration frequency analysis of three-layered cylinder shaped shell with effect of FGM central layer thickness, Scientific Reports, 2019, 9, 1566. doi:10.1038/s41598-018-38122-0
[23] Sanders Jr J.L., An improved first-approximation theory for thin shells, NASA Rep. (1959)
[24] Chi S.H. and Chung Y.L., Mechanical behavior of functionally graded material plates under transverse load part II: numerical results, Int. J. Solids Struct., 2006, 43, 3657–3691.

Appendix

$$K_{11} = \alpha^2\beta^2 x_{11} I_1 + n^2\beta^2(x_{66} - \beta y_{66} + \beta^2 z_{66}/4) I_2$$

$$K_{12} = -n\alpha\beta^2(x_{12} + \beta y_{12}) I_3 + n\alpha\beta^2(x_{66} + \beta y_{66} - 3\beta^2 z_{66}/4) I_4$$

$$K_{13} = \alpha\beta(x_{12} + n^2\beta y_{12}) I_5 + n^2\alpha\beta^2(-2y_{66} + \beta z_{66}) I_6 - \alpha^3\beta^2 y_{11} I_7$$

$$K_{22} = n^2\beta^2(x_{22} + 2\beta y_{22} + \beta^2 z_{22}) I_8 + \alpha^2\beta^2(x_{66} + 3\beta y_{66} + 9\beta^2 z_{66}/4) I_9$$

$$K_{21} = K_{12}$$

$$K_{23} = -n\beta(x_{22} + (n^2+1)\beta y_{22} + n^2\beta^2 z_{22}) I_{10} - n\alpha^2\beta^2(2y_{66} + 3\beta z_{66}) I_{11} + n\alpha^2\beta^2(y_{12} + \beta z_{12}) I_{12}$$

$$K_{31} = K_{13}$$

$$K_{32} = K_{23}$$

$$K_{33} = (x_{22} + 2n^2\beta y_{22} + n^4\beta^2 z_{22}) I_{13} + 4n^2\alpha^2\beta^2 z_{66} I_{14} - \alpha^2\beta(y_{12} + n^2\beta z_{12}) I_{15} + \alpha^4\beta^2 z_{11} I_{16}$$

where

$$I_1 = \int_0^L \left(d\underline{U}/dX\right)^2 dX,\; I_2 = \int_0^L \underline{U}^2 dX,$$

$$I_3 = \int_0^L \left(d\underline{U}/dX\right) \underline{V} dX,\; I_4 = \int_0^L \left(d\underline{V}/dX\right) \underline{U} dX,$$

$$I_5 = \int_0^L \left(d\underline{U}/dX\right) \underline{W} dX,\; I_6 = \int_0^L \underline{U}\left(d\underline{W}/dX\right) dX,$$

$$I_7 = \int_0^L \left(d\underline{U}/dX\right)\left(d^2\underline{W}/dX^2\right) dX,$$

$$I_8 = \int_0^L \underline{V}^2 dX,\; I_9 = \int_0^L \left(d\underline{V}/dX\right)^2 \underline{U} dX,$$

$$I_{10} = \int_0^L \underline{VW} dX,\; I_{11} = \int_0^L \left(d\underline{V}/dX\right)\left(d\underline{W}/dX\right) dX,$$

$$I_{12} = \int_0^L \underline{V}\left(d^2\underline{W}/dX^2\right) dX,\; I_{13} = \int_0^L \underline{W}^2 dX,$$

$$I_{14} = \int_0^L \left(d\underline{W}/dX\right)^2 dX$$

$$I_{15} = \int_0^L 2\left(d^2\underline{W}/dX^2\right) \underline{W} dX,$$

$$I_{16} = \int_0^L \left(d^2\underline{W}/dX^2\right)^2 dX,$$

$$x_{11} = \frac{2E}{3(1-\mu^2)} + \frac{1}{(1-\mu_1^2)}\left[\frac{E_1 - E_2}{3(N+1)} + \frac{E_2}{3}\right]$$

$$x_{12} = \frac{2E\mu}{3(1-\mu^2)} + \frac{\mu_1}{(1-\mu_1^2)}\left[\frac{E_1 - E_2}{3(N+1)} + \frac{E_2}{3}\right]$$

$$x_{66} = \frac{E}{3(1+\mu)} + \frac{1}{2(1+\mu_1)}\left[\frac{E_1 - E_2}{3(N+1)} + \frac{E_2}{3}\right]$$

$$x_{22} = x_{11}$$

$$x_{11} = \frac{2E}{3(1-\mu^2)} + \frac{1}{(1-\mu_1^2)}\left[\frac{E_1 - E_2}{3(N+1)} + \frac{E_2}{3}\right]$$

$$x_{12} = \frac{2E\mu}{3(1-\mu^2)} + \frac{\mu_1}{(1-\mu_1^2)}\left[\frac{E_1 - E_2}{3(N+1)} + \frac{E_2}{3}\right]$$

$$x_{66} = \frac{E}{3(1+\mu)} + \frac{1}{2(1+\mu_1)}\left[\frac{E_1 - E_2}{3(N+1)} + \frac{E_2}{3}\right]$$

$$x_{22} = x_{11}$$

$$y_{11} = \frac{E_1 - E_2}{(1-\mu_1^2)}\left[\frac{1}{18(N+1)} + \frac{1}{9(N+1)(N+2)}\right]$$

$$y_{12} = \frac{\mu_1(E_1 - E_2)}{(1-\mu_1^2)}\left[\frac{1}{18(N+1)} + \frac{1}{9(N+1)(N+2)}\right]$$

$$y_{66} = \frac{(E_1 - E_2)}{2(1+\mu_1)}\left[\frac{1}{18(N+1)} + \frac{1}{9(N+1)(N+2)}\right]$$

$$y_{22} = y_{11}$$

$$z_{11} = z_{22} = \frac{13E}{162(1-\mu^2)} + \frac{E_1 - E_2}{(1-\mu_1^2)} \times \left[\frac{1}{108(N+1)} - \frac{1}{27(N+1)(N+2)} - \frac{2}{27(N+1)(N+2)(N+3)}\right] + \frac{E_2}{324(1-\mu_1^2)}$$

$$z_{12} = \frac{13\mu E}{162(1-\mu^2)} + \frac{\mu_1(E_1 - E_2)}{(1-\mu_1^2)} \times \left[\frac{1}{108(N+1)} - \frac{1}{27(N+1)(N+2)} - \frac{2}{27(N+1)(N+2)(N+3)}\right] + \frac{\mu_1 E_2}{324(1-\mu_1^2)}$$

$$z_{66}=\frac{13E}{324(1+\mu)}+\frac{E_1-E_2}{2(1+\mu_1)}\times\left[\frac{1}{108\,(N+1)}-\frac{1}{27\,(N+1)\,(N+2)}-\frac{2}{27\,(N+1)\,(N+2)\,(N+3)}\right]+\frac{E_2}{648(1+\mu_1)}$$

$$M_{11}=\beta^2 I_2,\ M_{22}=\beta^2 I_8, M_{33}=I_{13}$$
$$M_{12}=M_{13}=M_{21}=M_{23}=M_{31}=M_{32}=0$$